GENERALIZED PHASE STABILITY IN MULTIPACTING

Valery Shemelin
Laboratory for Elementary Particle Physics, Cornell University, Ithaca, NY 14853, USA

INTRODUCTION

The known theory of the multipactor discharge in a flat gap [1, 2] explains existence of borders of multipacting bands, or zones. Different bands correspond to different orders of the discharge. The borders of the bands are related either to the condition of stability or to the minimal or maximal energy when the secondary emission yield becomes equal to 1.

The literature on the subject of multipacting is quite extensive, but, as a rule, these papers usually deal with more complicated situations than a simple flat gap with homogeneous electric field.

Nevertheless, even accurate analytical computations for this simple case of multipacting show some discrepancy with experimental results. Usually, one considers this discrepancy to be connected to unknown in detail distribution of initial velocities of secondary electrons, some uncertainties in the secondary emission yield, to the experimental errors and so on.

The influence of the normal and tangential components of the initial velocity on the position of discharge bands was analyzed in [3] and [4]. Some considerations were taken into account for those starting phases when the decelerating field can return the electron to the same electrode from where it started. However, the difference between calculated and measured borders has remained significant.

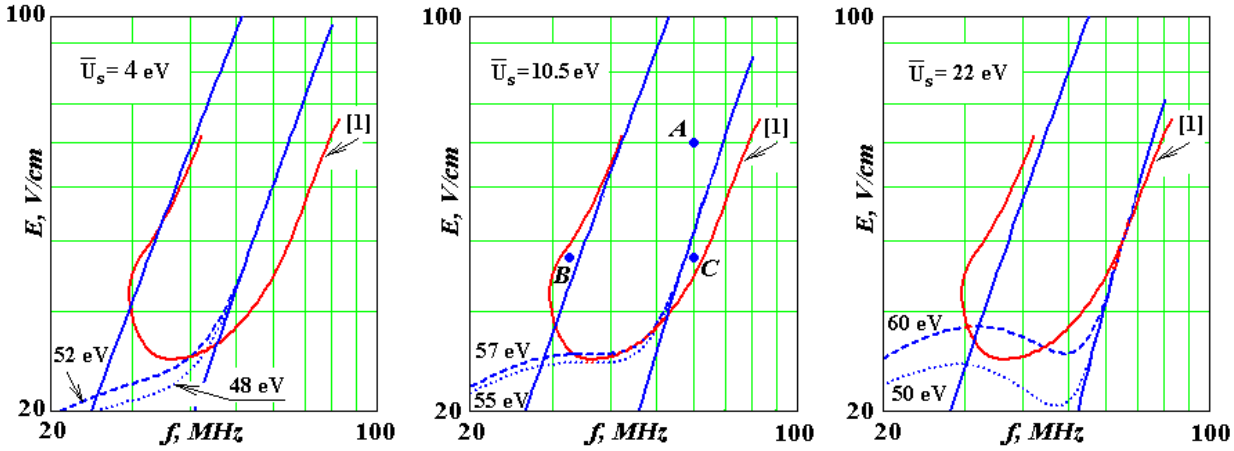

Fig. 1. Experimental curve [1] and calculated borders of the multipactor zone for different values of the initial energy $\overline{U}_s$ of secondary electrons. Straight solid lines are obtained from the condition of stability, dashed and dotted lines correspond to a border with SEY = 1 with different impact energy.

As an example of such a discrepancy we will analyze the experimental results of a pioneer paper by A. Hatch and H. Williams [1] taking into account conditions of stability and limitations by low impact energy. In the original work the condition of stability was presented for the motion that looked like reflection from the walls with a certain elasticity coefficient. But such a reflection does not correspond to experimental data. The value of the coefficient was just fitted to experiment.

On the experimental zone of multipacting, we will consider 3 points: *A*, *B*, and *C* (Fig. 1) where the discharge was observed. The earlier theory [3, 4] explains existence of discharge only in *A*.

In the present article generalization of the phase stability condition is proposed. The revised stability condition gives better understanding of the experimental results.

ANALYSIS OF THE EQUATION OF MOTION

The equation of motion for an electron in the gap is

$$\ddot{y} = \frac{eU}{md}\sin\omega t\,,$$

where the coordinate y is measured normal to the surface of one of the electrodes; e/m is the specific charge of the electron, the charge is considered positive to simplify the writing; U is the voltage across the gap, which is of the length d; $\omega = 2\pi f$, where f is the oscillation frequency; t

is the time. It is helpful to rewrite this in the normalized form [3]

$$\lambda'' = \xi \sin\theta\,, \qquad (1)$$

where $\lambda = y/d$, $\xi = U/U_0$, $U_0 = m\omega^2 d^2/e$, and $\theta = \omega t$; primes denote derivatives with respect to θ, while dots indicate derivatives with respect to *t*.

Integrating Eq. (1) we obtain

$$\lambda' = \xi(\cos\theta_1 - \cos\theta) + \beta_1\,, \qquad (2)$$

$$\lambda = \xi(\theta - \theta_1)\cos\theta_1 + \xi(\sin\theta_1 - \sin\theta) + \beta_1(\theta - \theta_1)\,. \qquad (3)$$

Here θ_1 is the phase at which the electron enters the gap, and $\beta_1 = \bar{v}_\perp/\omega d$ is the dimensionless average normal component of the initial velocity of the secondary electron.

As it is shown in [3] and [4], the value of β_1 corresponds approximately to one half of the initial energy of secondary electrons and can be expressed as follows

$$\beta_1 = \frac{\bar{v}_\perp}{\omega d} = \frac{2}{3}\frac{\bar{v}}{\omega d} = \frac{2}{3}\sqrt{\frac{2\overline{U_s}}{U_0}}\,. \qquad (4)$$

Here, the factor of $2/3$ appears because of the angular distribution of the secondary electrons and $(2/3)^2 \approx 0.5$ leads from $\overline{U_s}$ to $\sim 0.5\overline{U_s}$ for the normal component.

The condition for the electron to "resonantly" cross the gap is that the transit time be equal to an odd multiple of half-period of the RF field. This ensures that newly generated secondary electrons see the same conditions relative to the phase of the field as their predecessors. Equation (3) implies that

$$1 = \xi(\theta_2 - \theta_1)\cos\theta_1 + \xi(\sin\theta_1 - \sin\theta_2) + \beta_1(\theta_2 - \theta_1) \qquad (5)$$

where θ_2 is the phase at which the electron reaches the second electrode at $\lambda = 1$. Since the transit time $\theta_2 - \theta_1 = (2n-1)\pi$, (5) gives

$$\xi = \frac{1 - (2n-1)\pi\beta_1}{(2n-1)\pi\cos\theta_1 + 2\sin\theta_1}\,. \qquad (6)$$

So, for each starting phase θ_1 we can find the value of normalized voltage ξ and hence voltage *U* across the gap. The discharge is possible at this voltage if the stability condition is satisfied. Usually, this means that the initial phase of next generations of electrons does not change significantly if the initial electron has an excursion of its phase. The excursion of the phase relative to the equilibrium phase will decrease with each crossing the gap under the condition

$$\left|\partial\theta_2/\partial\theta_1\right| < 1\,. \qquad (7)$$

We will call this the *simple stability condition*. Later we will introduce the conception of a *generalized stability condition.*

Analysis of the motion for the marked points *A*, *B*, and *C* could be performed right away, however we need to pay attention to the value β_1 defined earlier.

The most probable initial velocity of the secondary electron is usually associated with the peak of energy distribution of these electrons. However, it is wrong and because the initial energy $\overline{U_s}$ defines the value β_1, we will discuss this separately.

DISTRIBUTION OF INITIAL VELOCITIES AND THE BOUNDARY WITH SEY = 1

In the discussed experiment silver-plated electrodes were used. The energy distribution of secondary electrons for the case of silver electrodes can be taken from [5]. The expression for the energy distribution function

$$dn = f(W)dW$$

can be recalculated for initial velocities or, that is more convenient, for the variable of $\sqrt{W}$:

$$dn = f(mv^2/2)mvdv = 2\sqrt{W}\,f(W)d\sqrt{W}\,.$$

As it can be seen from Fig. 2, the distribution with respect to $\sqrt{W}$ has a well-defined maximum corresponding to the most probable velocity of the secondary electrons.

For calculation of this distribution, the original experimental data (Fig. 2, upper left) were presented analytically as

$$f(W) = 0.07 + p\cdot\exp\left(-\frac{W^n}{A}\right) - (p + 0.07)\exp\left(\frac{-W - 0.5W^2}{B}\right)$$

with p = 1.15, n = 1.05, A = 22, and B = 3. This gives the average value of the secondary electron energy as 22 eV and the most probable velocity corresponds to energy of 10.5 eV. We neglect here the elastically scattered electrons, who give the sharp maximum in Fig. 2, upper left picture.

In Fig. 1 the upper and lower borders of the 1st ($n = 1$) discharge zone are presented for different values of the initial energy (almost straight lines). These borders are obtained in [3] from the condition (7). Also shown are the curves for the energy bounds corresponding to SEY = 1. One can see that the curvature of the line showing the energy bound fits experimental data best for the initial energy of 10.5 eV *i.e.* for the most probable velocity. The

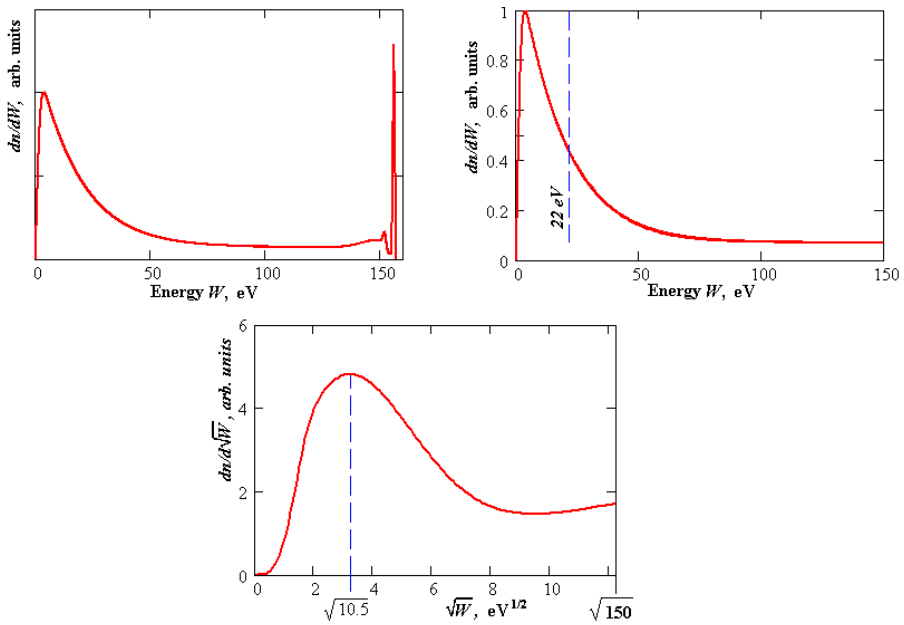

Fig. 2. Energy distribution of secondary electrons emitted by silver [5], its analytical approximation and distribution with respect to square root of energy.

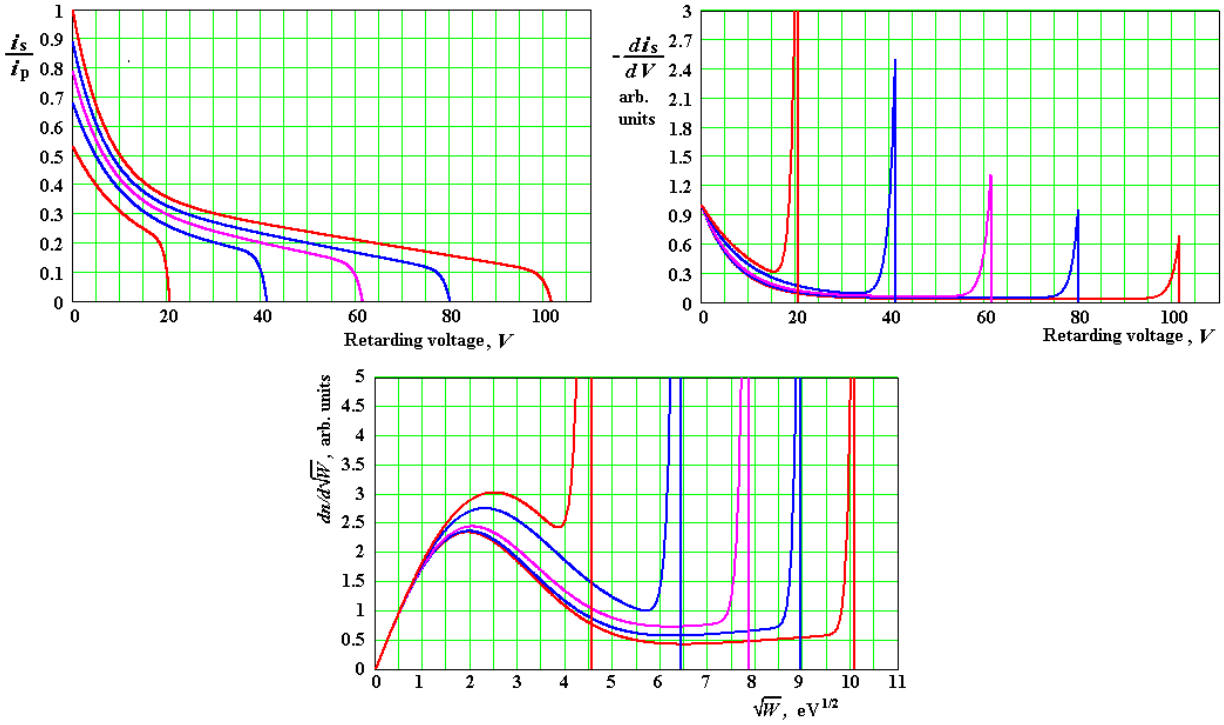

Fig. 3. Energy distribution of secondary electrons emitted by copper [5], its analytically obtained derivative and distribution with respect to square root of energy.

initial energy of secondary electrons of 4 eV used in earlier papers [3, 4] is presumably not consistent with this physical situation (see Fig. 1, left) though gives maximum in the energy distribution. The average value of energy, 22 eV (Fig. 1, right), also cannot be used.

However, the initial energy value $\overline{U_s} = 4$ eV appears to be correct if we analyze the copper electrodes. In Fig. 3, upper left, the experimental data [5] for copper are shown. Next two pictures present the mathematical handling of these data. It is clearly seen that for the initial energy of primary electrons 60…100 eV, the *velocity peak* position is close to 4 ÷ 6 eV. This data for copper (Fig. 3, upper right) reveals a peak of *energy* distribution at $V = 0$, not at $V = 4 \div 6$ volts as it is for silver (Fig. 2, both upper pictures), and the peak of reflected electrons is too broad in comparison with the previous data for silver. Both these features are determined by derivatives at the ends of curves. However, even if there are some experimental errors, the peak of velocity distribution at 4 eV is determined by the behavior of the middle part of these curves and can be treated as more or less reliable.

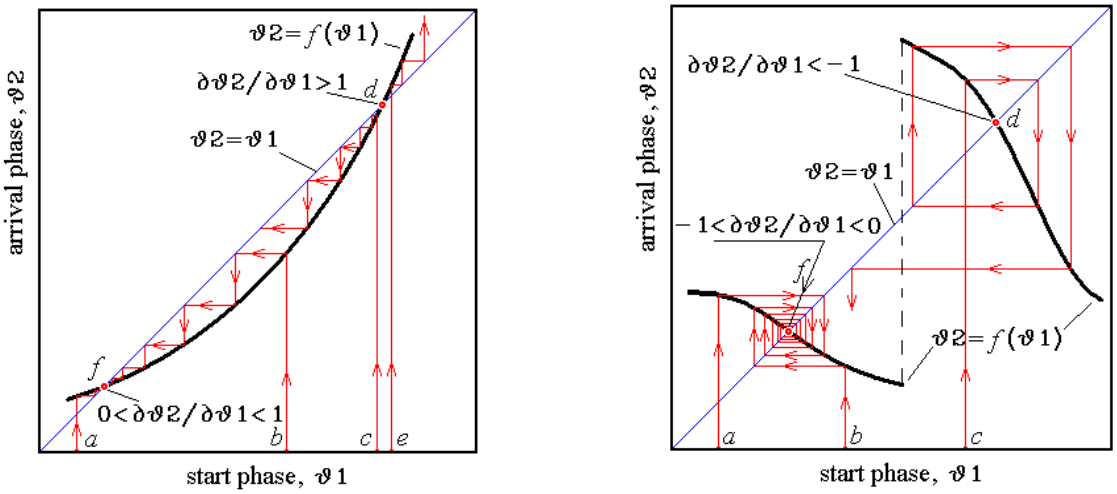

Fig. 4. Focusing to a stable phase and defocusing from an unstable phase for an increasing and a decreasing function $\theta_2 = f(\theta_1)$.

STABILITY CONDITIONS FOR DIFFERENT POINTS OF THE MULTIPACTING ZONE

The condition for the stable electron motion in a multipactor discharge requires that the electron enter the gap at a definite phase. We can use (6) to calculate the normalized voltage ξ at which the discharge exists for a given start phase.

The change in the phase at the exit from the gap is determined by fluctuations in the initial velocity and by the initial change in the phase at the entrance. Here we will neglect the initial velocity fluctuation: it is shown [3] that the same results are obtained if we take into account fluctuations in the initial phase only.

If the particle crosses the gap, the function $\theta_2 = f(\theta_1)$ can be obtained from (5). If the electron goes back to the same surface where it was emitted, the value of 1 in the left-hand side of (5) should be replaced by 0.

Let us introduce a simple graphic interpretation of phase motion, focusing and defocusing. With help of bisector of the right angle between coordinate axes we can easily find the starting phase for the next gap-crossing if we know the previous starting phase and if the function $\theta_2 = f(\theta_1)$ is defined.

The examples of phase motion of an electron in the gap are shown in Fig. 4. Four different cases of the value $\partial\theta_2/\partial\theta_1$ used in (7) are shown in the picture. It is arbitrarily assumed for this figure that the secondary electron yield SEY = 1. Focusing (*f*) and defocusing (*d*) points are shown for positive (left picture) and negative (right) values of $\partial\theta_2/\partial\theta_1$.

Let us subtract the integer odd number of π radians from the phase θ_2 if the particle crosses the gap and subtract the even number of π radians from this phase if the particle falls on the same electrode it was emitted from. Let these integer numbers be such that the phases of arrival are in the interval $[-\pi, \pi]$. Then the phase of the particle "in resonance" will be the same after crossing the

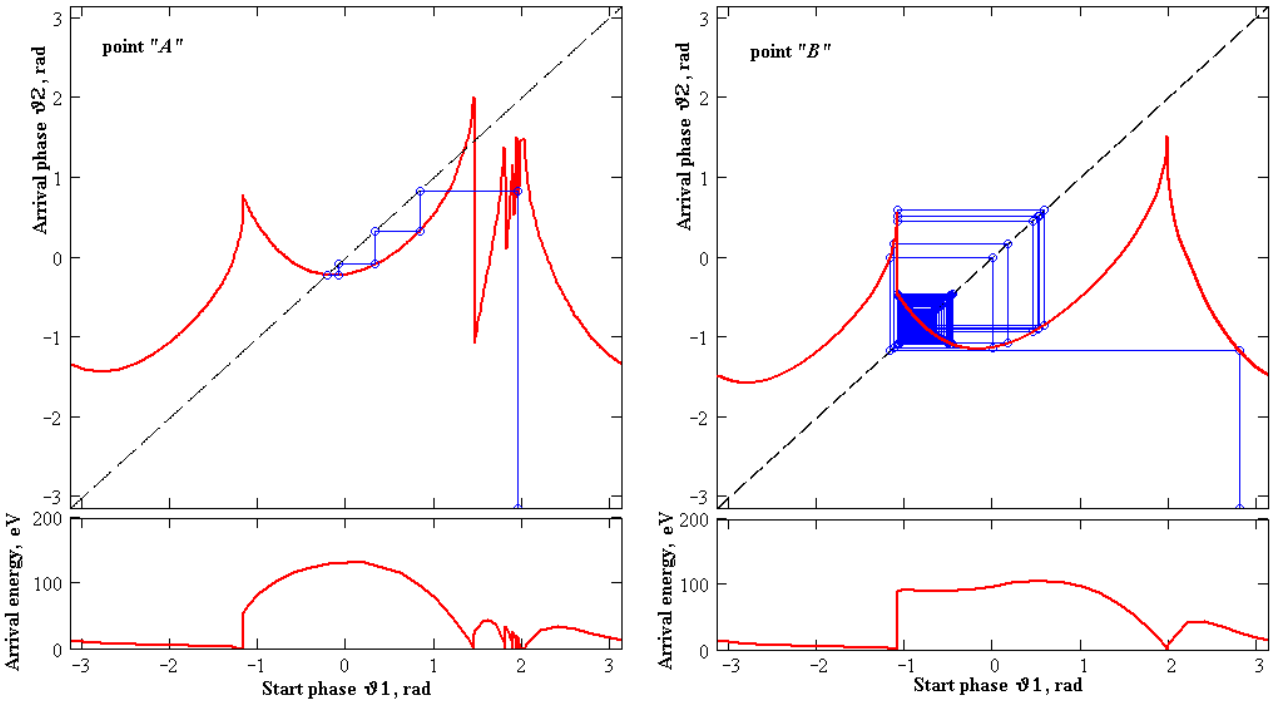

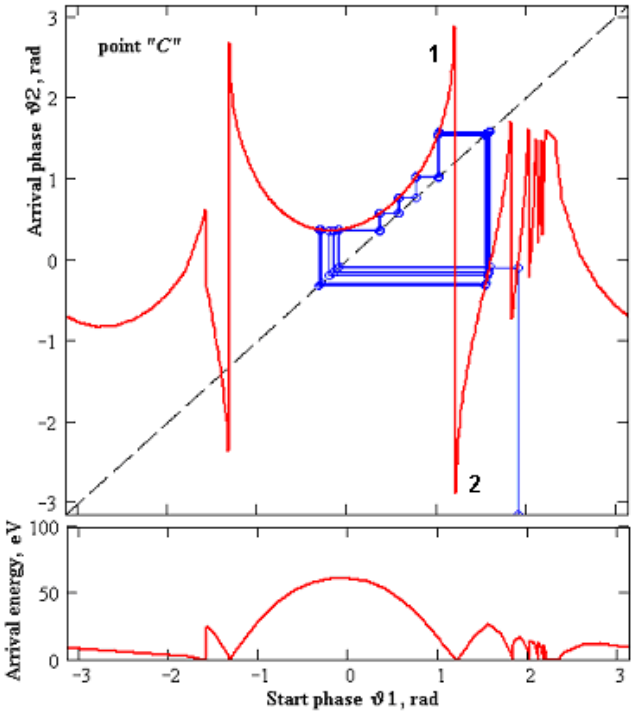

Fig. 5. Starting and arrival phases, and impact energy at arrival for the marked points of Fig. 1.

gap: $\theta_2 = \theta_1$. It is obvious that the condition of stability (7) will not change after such a transformation of θ_2. The advantage of this transformation lies in the fact that both phases, θ_1 and θ_2, are now placed on the limited intervals, and the graphical interpretation of the phase motion becomes very illustrative.

Now, when we have defined the value of β_1 and redefined θ_2, we can return to construction of the function $\theta_2 = f(\theta_1)$ for points *A*, *B*, and *C* of Fig. 1. This function, the phase trajectory for an arbitrary initial starting phase, and the corresponding impact energy are presented in Fig. 5. For each of three points 100 flights of the particle are calculated. It is assumed again that neither generation of new electrons nor loss of them occurs on the surface (SEY = 1).

The case of the point *A* is very simple. The condition (7) is satisfied for $\theta_1 = -0.227$. After 5 crossings of the gap the particle settles down to the focus point and all next phase positions coincide. Impact energy at this point is high enough, about 130 eV (see the lower part of the picture), to produce secondary electrons with SEI > 1. So it is a point of multipacting.

The simple stability condition is not satisfied in the point *B* because $\partial\theta_2/\partial\theta_1 = -1.09 < -1$. Let us distinguish two squares on the picture for this case. The inner one is tightly hatched because though defocusing process develops, the value of the derivative is not too high and lines go close one to another. The other one is the maximal square on the bisector the upper side of which is shown on the Fig. 5 for the point *B* (*MNPQ* in Fig. 6). The pattern of the phase trajectory practically doesn't depend on the initial start phase. When the phase trajectory reaches the point *M* (see details in Fig. 6), its continuation enters again into the smaller square. This trajectory cannot quit the square *MNPQ* as can be seen from Fig. 6, because after any small

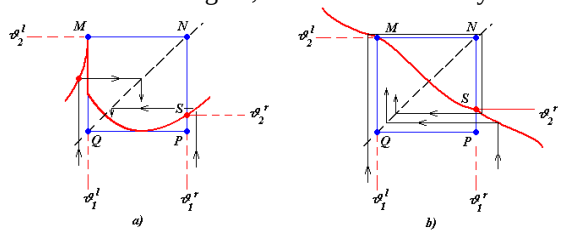

Fig. 6. A square of stability for the case *B*.

deviation of the trajectory outside the square, it enters again into this square. The necessary condition for this is that the entire curve $\theta_2 = f(\theta_1)$ is inside the square. Fig. 6a shows the same situation that in Fig. 5 for point *B*; in Fig. 6b another possible behavior of the function $f(\theta_1)$ is shown: without a jump of the derivative at θ_1^l. We can formulate the 1st condition of the generalized stability: if a part of the curve $\theta_2 = f(\theta_1)$ can be placed inside a square located on the bisector of coordinate axes θ_1, θ_2 as on the diagonal, and the values corresponding to the left and right sides of this square are θ_1^l and θ_1^r, and the related values θ_2^l and θ_2^r satisfy the ratio

$$\left|\frac{\theta_2^r - \theta_2^l}{\theta_1^r - \theta_1^l}\right| < 1, \qquad (8)$$

the motion is finite and limited by phase angles θ_1^l and θ_1^r. The simple condition of stability (7), as can be easily seen, is a particular case of (8).

The whole curve defined on the interval $[-\pi, \pi]$ always satisfies condition (8) but it doesn't make special physical sense, just presents another limiting case.

The case of the point *C* is a case of a repetitive motion when part of the curve $\theta_2 = f(\theta_1)$ escapes from the square (peaks 1 and 2, Fig. 5) but the whole trajectory stays within a limited interval. For description of this motion let us introduce "higher order" functions:

$$\theta_3 = f_2(\theta_1) = f(f(\theta_1)),\ \theta_4 = f_3(\theta_1) = f(f_2(\theta_1)),\ \ldots$$
$$\theta_{m+1} = f_m(\theta_1) = f(f_{m-1}(\theta_1)). \qquad (9)$$

It appears for the motion presented in Fig. 5, point *C*, that the equation

$$f_m(\theta_1) = \theta_1 \qquad (10)$$

has a solution for $m = 6$. So the motion repeats after 6 different start phases. This motion could be stable if

$$\left|\partial f_m(\theta_1)/\partial\theta_1\right| < 1, \qquad (11)$$

$m = 6$ for the point *C*. However, the inequality (11) is not satisfied in this case: $\partial\theta_7/\partial\theta_1 = -3.86$. Nevertheless, because of the particular pattern of the phase trajectory, no particle falls into the region of peaks 1 and 2 (see Fig. 5, point *C*). And for the outlined square the same condition (8) is valid as for the point *B*.

The inequality (11) together with the condition (10) can be treated as the second generalized condition of stability. It reduces to the case of the simple stability condition (7), when *m* is equal to 1. We should assume $f_1(\theta_1) \equiv f(\theta_1)$ in this case.

Another presentation of the phase motion is shown in Fig. 7. Here the starting phase θ_m is plotted versus the number of the flight.

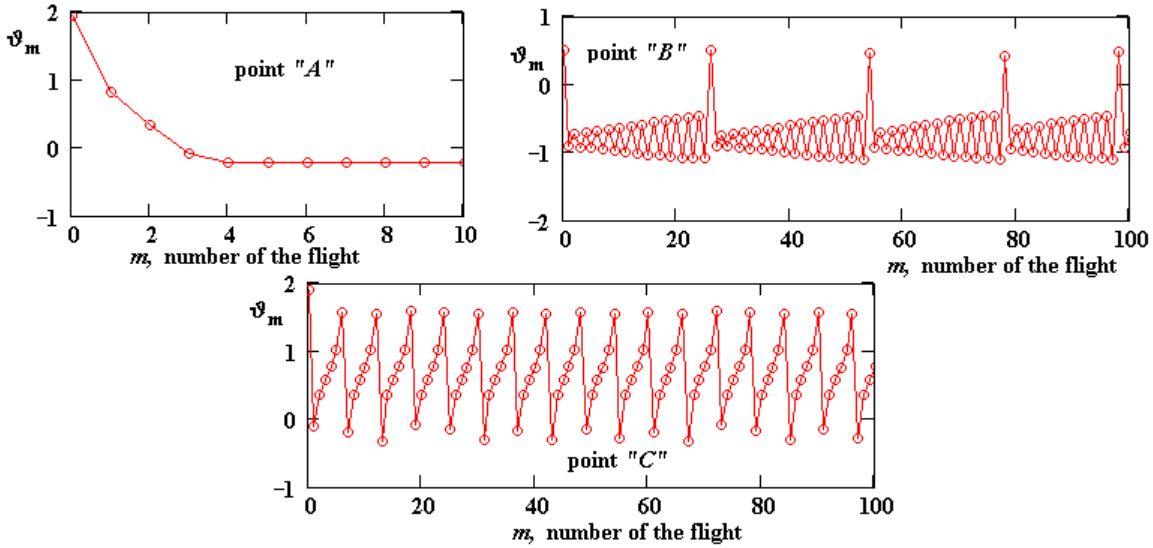

Fig. 7. Dependence of the starting phase on the number of the flight.

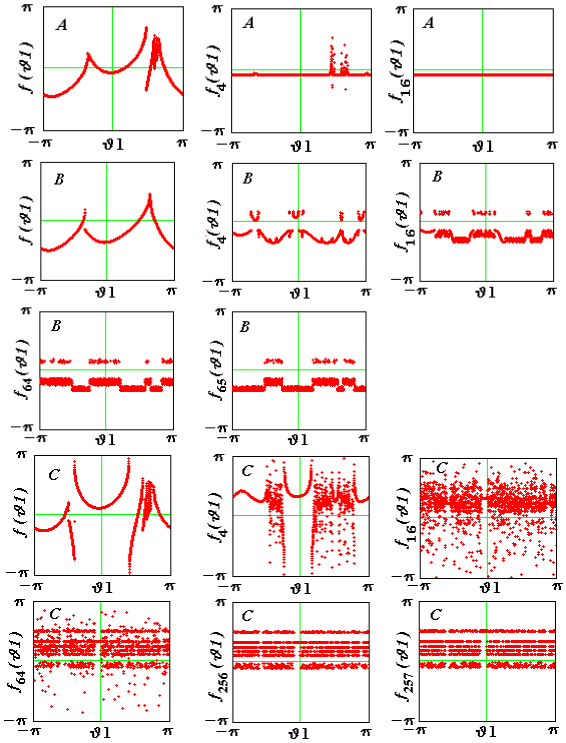

Fig. 8. Phase portrait of multipacting for points *A*, *B*, and *C* of Fig. 1 after different number of flights.

One more description of the grouping process is shown in Fig. 8. Here for the initial phase θ_1 homogeneously distributed in the interval $[-\pi,\pi]$ (1000 points), the next generations of particles are shown after different number of flights. Two last pictures for points *B* and *C* show a change of phase for two successive flights.

CONCLUSIONS

Introduction of the generalized condition of stability in multipacting helps to understand the expanding of multipacting zones beyond the limits predicted by the simple stability condition. The illustrative phase diagram for a flat gap shows the phase motion when the simple condition of stability is both applicable and not applicable for description of motion. Other presentations of the grouping process show that the electrons of the multipactor discharge can group into layers even when the simple condition of stability doesn't work.

The results of this work are applicable for more complicated geometries when experimental zones appear broader than obtained by simulations [6].

Results obtained for initial velocities of secondary electrons should be taken into account in simulations.

Further analysis of the multipacting phenomena in a flat gap is in progress. In particularly, it is intended to analyze the influence of the secondary emission yield and obtain theoretical boundaries of the zones taking into account all possible cases of motion.

The author is grateful to Sergey Belomestnykh for useful discussions.

REFERENCES

1. *A.J. Hatch, H.B. Williams.* The secondary electron resonance mechanism of low-pressure high-frequency gas breakdown. J. Appl. Phys., **25,** 417 (1954).

2. *A.J. Hatch, H.B. Williams.* Multipacting modes of high-frequency gaseous discharge. Phys. Rev. **112,** 681 (1958).
3. *V.D. Shemelin.* Existence zones for multipactor discharges. Sov. Phys. Tech. Phys. **31** (9), September 1986.
4. *V.D. Shemelin.* Multipactor discharge in a rectangular waveguide with regard to normal and tangential velocity components of secondary electrons. Cornell University LNS report SRF 010322-03. 2001.
5. *H. Bruining.* Physics and applications of secondary electron emission. London, Pergamon Press, 1954.
6. *R.L. Geng et al.* Suppression of multipacting in rectangular coupler waveguides. Cornell University LNS report SRF 030520-15. 2003.